NACA

RESEARCH MEMORANDUM

TRANSONIC WIND-TUNNEL INVESTIGATION OF THE AERODYNAMIC LOADING CHARACTERISTICS OF A HIGHLY TAPERED UNSWEPT WING IN THE PRESENCE OF A BODY WITH AND WITHOUT INDENTATION

By Joseph D. Brooks

Langley Aeronautical Laboratory
Langley Field, Va.

[redacted]

NATIONAL ADVISORY COMMITTEE
FOR AERONAUTICS

WASHINGTON

February 1, 1956

[redacted]

Classification cancelled (or changed to Unclassified)

By authority of NASA Tech Pub Announcement #121
(OFFICER AUTHORIZED TO MAKE CHANGE)

By 4 Nov 75

GRADE OF OFFICER MAKING CHANGE)

30 March 81
DATE

NATIONAL ADVISORY COMMITTEE FOR AERONAUTICS

RESEARCH MEMORANDUM

TRANSONIC WIND-TUNNEL INVESTIGATION OF THE AERODYNAMIC LOADING CHARACTERISTICS OF A HIGHLY TAPERED UNSWEPT WING IN THE PRESENCE OF A BODY WITH AND WITHOUT INDENTATION

By Joseph D. Brooks

SUMMARY

A transonic investigation of the aerodynamic loading characteristics and the effects of body indentation on the wing loads of a low-aspect-ratio, highly tapered, unswept wing in the presence of a body has been conducted in the Langley 8-foot transonic pressure tunnel. The tests covered a range of Mach numbers from 0.60 to 1.20 for angles of attack from 0° to 20°.

The results show that with increasing normal-force coefficient at Mach numbers up to 0.88 the center of pressure moves abruptly rearward and slightly inboard following separation. Above a Mach number of 0.88, separation is not evident within the range of the data presented. With increasing Mach number through the transonic speed range, the center of pressure moves rearward very rapidly, while it moves slowly inboard. The location of the center of pressure of the wing with the indented body is generally rearward and slightly inboard of that of the wing with the basic body. The results of a theoretical calculation of the lateral center-of-pressure location at a Mach number of 1.41 agree with the experimental data at the lower supersonic Mach numbers of 1.05 to 1.20.

INTRODUCTION

A general investigation to determine the effects of wing geometry and body indentation on wing loads at transonic speeds has been conducted in the Langley 8-foot transonic pressure tunnel. The effects of taper ratio and body indentation with a 45° sweptback wing have been reported in reference 1 and the effects of sweepback and thickness

ratio in reference 2. The purpose of this paper is to show the aerodynamic loading characteristics of a low-aspect-ratio, highly tapered, unswept wing in the presence of a body and the effects of body indentation on the wing loads. Since force test data are available in reference 3 for the total load on the same wing-body combinations, the division of normal-force and pitching-moment load between the wing and the body was also determined.

The unswept wing tested has a taper ratio of 0.2, aspect ratio of 2.67, and 4-percent-thick circular-arc airfoil sections measured parallel to the plane of symmetry. The wing was tested in the presence of a basic body and a body indented according to the transonic area rule of reference 4.

Normal force, pitching moment, and bending moment of the wing were measured by means of a strain-gage balance. From these measurements, the location of the wing center of pressure was computed.

SYMBOLS

b	span of wing
C_B	bending-moment coefficient for wing panel, $\frac{M_B}{q\frac{S}{2}\frac{b}{2}}$
C_{m_W}	pitching-moment coefficient of wing in presence of body $M_W/qS\bar{c}$
$C_{m_{WB}}$	pitching-moment coefficient of wing-body combination $M_{WB}/qS\bar{c}$
C_{N_W}	normal-force coefficient for wing in presence of body, N_W/qS
$C_{N_{WB}}$	normal-force coefficient on wing-body combination, N_{WB}/qS
c	section chord of wing measured parallel to plane of symmetry of model
$\bar{c}$	wing mean aerodynamic chord, $\frac{2}{S}\int_0^{b/2} c^2 dy$
c.p.	wing center of pressure
M	free-stream Mach number

[redacted]

M_B bending moment for a wing panel about fuselage center line

M_W pitching moment of wing in presence of body, about $0.25\bar{c}$

M_{WB} pitching moment of wing-body combination about $0.25\bar{c}$

N_W normal force on wing in presence of body

N_{WB} normal force on wing-body combination

q free-stream dynamic pressure, $\rho V^2/2$

R Reynolds number, $\rho V\bar{c}/\mu$

S total wing area

t maximum section thickness

V free-stream velocity

$x/\bar{c}$ longitudinal location of center of pressure in terms of mean aerodynamic chord, measured from leading edge of mean aerodynamic chord, $0.25 - \frac{C_{m_W}}{C_{N_W}}$

y lateral distance from the model plane of symmetry to wing center of pressure

$\frac{y}{b/2}$ lateral location of center of pressure, in terms of wing semispan, measured from fuselage center line, C_B/C_{N_W}

α angle of attack of model measured from fuselage center line, deg

μ coefficient of viscosity in free stream

ρ mass density in free stream

APPARATUS AND METHODS

Tunnel

The test section of the Langley 8-foot transonic pressure tunnel is rectangular in cross section. The upper and lower walls of the test section are slotted to allow continuous operation through the transonic speed range. Some details of the test section are shown in figure 1. The sting support system shown in figure 1 was designed to keep the model near the center line of the tunnel throughout the angle-of-attack range.

During this investigation, the tunnel was operated at approximately atmospheric stagnation pressure and the stagnation temperature was automatically controlled and held constant at 120° F. The tunnel air was dried sufficiently to lower the dewpoint temperature below 0° F in order to prevent the formation of condensation shocks.

The tunnel was calibrated by means of an axial survey tube, provided with static-pressure orifices along its length, which extended from the entrance cone to the beginning of the diffuser. Some representative axial Mach number distributions at the center of the tunnel are shown in figure 2. The flow in the vicinity of the wing was satisfactorily uniform at all test Mach numbers. Local deviations from the average stream Mach number were no larger than 0.005 at subsonic speeds. With increases in Mach number above 1.0, these deviations increased but did not exceed 0.010 in the region of the wing at the highest test Mach number of 1.20.

Model

The plan form and dimensions of the wing tested are shown in figure 3. The wing had 0° sweepback of the quarter-chord line, an aspect ratio of 2.67, and a taper ratio 0.2. The wing was constructed of aluminum alloy and the airfoil sections parallel to the model plane of symmetry were 4-percent-thick symmetrical sections made up of circular arcs with the maximum thickness located at the 40-percent-chord station. The wing area was 0.96 square foot and the maximum cross-sectional area of the body is 0.077 square foot.

The body frame was constructed of steel and contained a strain-gage balance designed to measure wing loads independently of any body load. The balance measured bending moment on each wing and normal force and pitching moment for both wings. The wings were mounted in the balance, as shown in the detailed drawing of figure 3, and were independent of the body frame. A photograph of the balance in the body is shown in figure 4. The outer body shell was independent of the balance and the body shape could be changed between stations 22.5 and 37.5. The wing

was tested in the presence of a basic and also an indented body. The shape of the indented body was obtained according to the transonic area rule for a Mach number of 1.0 (ref. 4). Photographs of the complete model showing the wing in the presence of the basic and the indented bodies are shown in figures 5 and 6, respectively. The coordinates of the basic and indented bodies are given in table I.

A gap of about 0.030 inch was left between the outer body shell and the wing to prevent fouling of the wing on the body. For the tests of the wing in the presence of the basic body, the gap between the wing and outer body shell was sealed with soft rubber tubing, as shown in the detailed drawing of figure 3. However, for the tests of the wing in the presence of the indented body, the gap was not sealed because the outer body shell was not thick enough to permit the use of seals. The addition of the rubber seals decreased the strain-gage-balance sensitivity as much as 5 percent. For this reason, the balance was recalibrated before the test of the sealed configuration. For all tests the hollow sting was plugged at the base of the model to prevent any flow through the sting.

The angle of attack was measured by a strain-gage attitude transmitter. The instrument was mounted in the body frame ahead of the wing.

Tests

The angle-of-attack range extended in most cases from 0° to 20°. At Mach numbers 0.91 and 0.94, the angle of attack was limited to maximum angles of 12° and 15°, respectively, by severe buffeting. The Mach number range extended from 0.60 to 1.20. Data were not recorded in the Mach number range between 1.03 and 1.12, since in this range the data may have been affected by reflections of the fuselage bow wave from the tunnel walls. The variation of Reynolds number (based on a mean aerodynamic chord of 8.267 inches) with Mach number is shown in figure 7.

Accuracy

The accuracy of the strain-gage measurements is estimated to be as follows:

M	Accuracy of -		
	C_{N_W}	C_{m_W}	C_B
0.60	±0.009	±0.004	±0.008
1.20	±.004	±.002	±.004

[redacted]

The average stream Mach number was held within ±0.003 of the nominal value given in the figures. The model angle of attack is estimated to be correct within ±0.1°.

As previously mentioned, the gap between the wing and the outer body shell was not sealed for the tests of the wing in the presence of the indented body. The effect of such a gap was investigated for two wings with 45° of sweepback and is shown in reference 1. For these wings, the data obtained with and without the seal were generally in good agreement at angles of attack below the point where the unstable break in the pitching-moment curve occurred.

The longitudinal and lateral position of the center of pressure on the wing was computed from faired curves of C_{m_W} against C_{N_W} and C_B against C_{N_W}, respectively. At some Mach numbers, these curves did not pass through the origin. Since the models were symmetrical about the horizontal plane passing through the center line of the model, the curves were shifted slightly to pass through the origin when the center-of-pressure locations were computed.

RESULTS AND DISCUSSION

Basic Aerodynamic Characteristics

The variation of angle of attack, pitching-moment coefficient, and bending-moment coefficient with wing normal-force coefficient for the wing in the presence of the basic and indented bodies is presented in figures 8 and 9, respectively. The bending-moment coefficients for both the left- and right-wing panels are shown in figures 8(c) and 9(c), flags on the symbols indicating the left-wing panel moment.

At Mach numbers from 0.60 to 0.88, the pitching-moment data (figs. 8(b) and 9(b)) show that the wing experiences rapid changes in pitching moment with increasing normal-force coefficient. These changes in pitching moment are associated with flow separation on the wing upper surface in a region near the leading edge. Separation occurs gradually at the low Mach numbers and with increasing Mach number occurs more abruptly and is also delayed to higher normal-force coefficients. At Mach numbers 0.91 and 0.94 the normal-force coefficient was limited by severe buffeting but separation is not evident within the range of the data presented. At Mach numbers above 0.94 the flow over the upper surface is probably completely supersonic, and apparently no separation occurs. This type of flow phenomena has been observed in two-dimensional data on unswept airfoils in reference 5 and in reference 6 on an unswept wing with an aspect ratio of 4.

Basic Center-of-Pressure Characteristics

The longitudinal and lateral variation of the center-of-pressure position with normal-force coefficient is presented in figure 10, and the variation with Mach number is presented in figure 11. The data of figure 10 indicate that with increasing normal-force coefficient the center of pressure, in general, shows only a rearward movement preceding separation. Separation is evident in the Mach number range from 0.60 to 0.88. When separation occurs, the center of pressure moves abruptly rearward and slightly inboard. As the Mach number increases, the data of figure 10 indicate that separation is delayed to higher normal-force coefficients. At Mach numbers above 0.88, separation is not evident within the range of the data presented and the longitudinal center of pressure moves generally rearward with increasing normal-force coefficient. There is little variation of the lateral center-of-pressure position with normal-force coefficient at these higher Mach numbers.

In figure 11, at constant normal-force coefficients up to 0.40, as the Mach number increases above 0.60, the center of pressure first experiences a gradual forward and outboard movement. Between the Mach numbers 0.85 and 1.0, the flow becomes supersonic on the wing upper surface and the center of pressure moves rearward very rapidly while moving slowly inboard. Above a Mach number of 1.0, the center of pressure continues to move rearward at a reduced rate and slightly inboard with increasing Mach number.

At a normal-force coefficient of 0.50, (fig. 11), the flow is separated on the upper surface of the wing near the leading edge between the Mach numbers 0.60 and 0.80 and the center of pressure is in a rearward and slightly inboard position. Between the Mach numbers 0.80 and 0.90, the flow reattaches and the center of pressure moves abruptly forward and slightly outboard. Above a Mach number of approximately 0.90 at constant normal-force coefficients of 0.50 and above, the center-of-pressure movement with increasing Mach number is generally the same as at the lower normal-force coefficients.

Effect of Body Indentation

The effect of body indentation on the center-of-pressure location is also shown in figures 10 and 11. The center of pressure for the wing in the presence of the indented body is generally 1 to 3 percent of the wing mean aerodynamic chord rearward and 1 to 2 percent of the wing semispan inboard of that for the wing with the basic body. This effect of body indentation is due largely to the inboard wing area that is exposed when the body is indented for a low-aspect-ratio unswept wing. Comparison of these results with those for 45° sweptback wings of aspect ratio 4 (ref. 1) shows that the effect of body indentation on center-of-pressure location is less for the wings of higher aspect ratio. This is to be

[redacted]

expected since body indentation is shown in reference 7 to affect primarily the wing pressures near the body.

In figure 11, at constant normal-force coefficients up to 0.40, another effect of body indentation is to delay slightly the Mach number at which the transonic rearward movement of the center of pressure begins. The same effect of body indentation was noted in reference 1.

Division of Load Between the Wing and Body

The division of load between the wing and body was determined from an analysis of the data presented herein and the data from reference 3. The indented body of reference 3 differs slightly from that used in the present investigation (table I); however, the differences are small and would not significantly affect the comparisons presented. The results are presented in figures 12 and 13.

Figure 12 shows the division of normal-force load for the wing in the presence of the body C_{N_W} as the ratio of $C_{N_W}/C_{N_{WB}}$ plotted against total normal-force coefficient $C_{N_{WB}}$. Also shown in figure 12 is the normal-force load of the body plus wing interference C_{N_B} as the ratio of $C_{N_B}/C_{N_{WB}}$ plotted against $C_{N_{WB}}$. The effects of Mach number and body indentation are obscured by the scatter in the data; however, the percentage of the total load that the wing carries generally increases slightly as the total normal-force coefficient increases.

The division of pitching-moment load is shown in figure 13 as the variation of pitching-moment coefficient for the wing-body combination and for the wing in the presence of the body against wing-body normal-force coefficient. Data for the basic and indented bodies are presented in figure 13. Flags on the symbols indicate the wing in the presence of the body. For a given Mach number, the slopes of the pitching-moment curves are more positive for the wing-body combination than for the wing in the presence of the body. With increasing Mach number, the difference in the slopes of the pitching-moment curves decreases.

Comparison With Theory

Results of a theoretical calculation of the lateral location of the center of pressure are shown in figure 14 with the experimental data obtained on the wing in the presence of the basic body at $C_{N_W} = 0.30$. No corrections were made to the theoretical spanwise distributions for body interference, and only the distributions outboard of the body

maximum radius were considered in the calculations. The theoretical additional loadings at subsonic speeds were obtained from the charts of reference 8 and at the supersonic speed from the equations of reference 9.

The comparison of the theoretical values with the experimental data is very good at subsonic speeds. At supersonic speeds, the theoretical point was calculated at the lowest Mach number ($M = 1.41$) at which the theory of reference 9 could be applied; however, this exceeds the highest test Mach number of 1.20. Since the theoretical point at the supersonic speed shows excellent agreement with the experimental data for lower supersonic speeds, it is concluded that the lateral center-of-pressure location at low supersonic speeds may be predicted from the theoretical value calculated for a higher Mach number. This conclusion is in general agreement with the conclusion of reference 2, which includes experimental data for a higher aspect-ratio, unswept wing and slightly thicker wings with sweepback angles of 0°, 35°, and 45°. In reference 1, the lateral center-of-pressure locations at low supersonic speeds for two 45° sweptback wings with taper ratios of 0.3 and 0.6 were also predicted in a similar manner using the equations of reference 10.

In calculating the lateral center-of-pressure location at supersonic speeds, it is necessary to determine the lowest Mach number at which the equations of references 9 and 10 can be applied. To do this, determine first the Mach number at which the Mach line is parallel to the trailing edge of the wing. Then determine the Mach number at which the Mach line is parallel to a line from the leading edge of the tip chord to the trailing edge of the theoretical root chord. The higher of these two Mach numbers is the lowest Mach number at which the equations of reference 9 or 10 can be used. For this Mach number determine the position of the Mach line from the leading edge of the root chord with respect to the leading edge of the wing. If the Mach line from the leading edge of the root chord is behind the leading edge of the wing, use reference 9 (for supersonic leading edge). If the Mach line is forward of the leading edge of the wing, use reference 10 (for subsonic leading edge).

CONCLUSIONS

An investigation, made in the Langley 8-foot transonic pressure tunnel, of the wing loads on a highly tapered, unswept wing in the presence of a basic and an indented body, leads to the following conclusions:

1. With increasing wing normal-force coefficient at a constant Mach number, the center of pressure moves slowly rearward until, at the subsonic Mach numbers from 0.60 to 0.88, separation occurs. At this point the center of pressure moves abruptly rearward and slightly inboard.

Above a Mach number of 0.88, separation is not evident within the range of the data presented and the center of pressure continues to move rearward with increasing wing normal-force coefficient.

2. With increasing Mach number at a constant wing normal-force coefficient below separation, the center of pressure experiences a gradual forward and outboard movement up to a Mach number of approximately 0.85. Between the Mach numbers of approximately 0.85 and 1.0, the induced velocities become supersonic and the center of pressure moves rearward very rapidly while it moves slowly inboard. Above a Mach number of 1.0, the center of pressure continues to move rearward at a reduced rate and slightly inboard.

3. The center of pressure of the wing with the indented body is generally rearward and slightly inboard of that of the wing with the basic body. Body indentation delays slightly the Mach number at which the transonic rearward shift of the center of pressure begins.

4. The result of a theoretical calculation of the lateral center-of-pressure location at a Mach number of 1.41 (the lowest Mach number at which the theory of NACA TN 2643 can be applied to this wing) agrees with the experimental data at lower supersonic Mach numbers of 1.05 to 1.20.

Langley Aeronautical Laboratory,
National Advisory Committee for Aeronautics,
Langley Field, Va., October 10, 1955.

REFERENCES

1. Delano, James B., and Mugler, John P., Jr.: Transonic Wind-Tunnel Investigation of the Effects of Taper Ratio and Body Indentation on the Aerodynamic Loading Characteristics of a 45° Sweptback Wing in the Presence of a Body. NACA RM L54L28, 1955.

2. Platt, Robert J., Jr., and Brooks, Joseph D.: Transonic Wind-Tunnel Investigation of the Effects of Sweepback and Thickness Ratio on the Wing Loads of a Wing-Body Combination of Aspect Ratio 4 and Taper Ratio 0.6. NACA RM L54L31b, 1955.

3. Kelly, Thomas C.: Transonic Wind-Tunnel Investigation of the Effects of Body Indentation for Boattail and Cylindrical Afterbody Shapes on the Aerodynamic Characteristics of an Unswept-Wing-Body Combination. NACA RM L54A08, 1954.

4. Whitcomb, Richard T.: A Study of the Zero-Lift Drag-Rise Characteristics of Wing-Body Combinations Near the Speed of Sound. NACA RM L52H08, 1952.

5. Lindsey, W. F., Daley, Bernard N., and Humphreys, Milton D.: The Flow and Force Characteristics of Supersonic Airfoils at High Subsonic Speeds. NACA TN 1211, 1947.

6. Hieser, Gerald, Henderson, James H., and Swihart, John M.: Transonic Aerodynamic and Loads Characteristics of a 4-Percent-Thick Unswept-Wing—Fuselage Combination. NACA RM L54B24, 1954.

7. Byrd, Paul F.: Theoretical Pressure Distributions for Some Slender Wing-Body Combinations at Zero Lift. NACA RM A54J07, 1955.

8. DeYoung, John, and Harper, Charles W.: Theoretical Symmetric Span Loading at Subsonic Speeds for Wings Having Arbitrary Plan Form. NACA Rep. 921, 1948.

9. Martin, John C., and Jeffreys, Isabella: Span Load Distributions Resulting From Angle of Attack, Rolling, and Pitching for Tapered Sweptback Wings With Streamwise Tips - Supersonic Leading and Trailing Edges. NACA TN 2643, 1952.

10. Hannah, Margery E., and Margolis, Kenneth: Span Load Distributions Resulting From Constant Angle of Attack, Steady Rolling Velocity, Steady Pitching Velocity, and Constant Vertical Acceleration for Tapered Sweptback Wings With Streamwise Tips - Subsonic Leading Edges and Supersonic Trailing Edges. NACA TN 2831, 1952.

[redacted]

TABLE I.- BODY COORDINATES

Forebody		Afterbody			
		Basic body		Indented body	
Station, in. from nose	Radius, in.	Station, in. from nose	Radius, in.	Station, in. from nose	Radius, in.
0	0	22.500	1.875	22.500	1.875
.225	.104	26.500	1.875	24.970	1.875
.5625	.193	27.692	1.868	25.500	1.855
1.125	.325	28.692	1.862	26.000	1.802
2.250	.542	29.692	1.849	27.000	1.626
3.375	.726	30.692	1.825	27.500	1.530
4.500	.887	31.692	1.789	28.000	1.498
6.750	1.167	32.692	1.745	28.500	1.494
9.000	1.390	33.692	1.694	29.000	1.504
11.250	1.559	34.692	1.638	30.000	1.545
13.500	1.683	35.692	1.570	31.000	1.592
15.750	1.770	36.692	1.486	32.000	1.634
18.000	1.828	36.900	1.468	33.000	1.657
20.250	1.864	37.500	1.408	34.000	1.651
		38.500	1.298	35.000	1.618
		39.500	1.167	36.000	1.548
		40.500	1.030	36.900	1.467
		41.250	.937	37.500	1.408
				37.500-41.250	Same coordinates as basic body

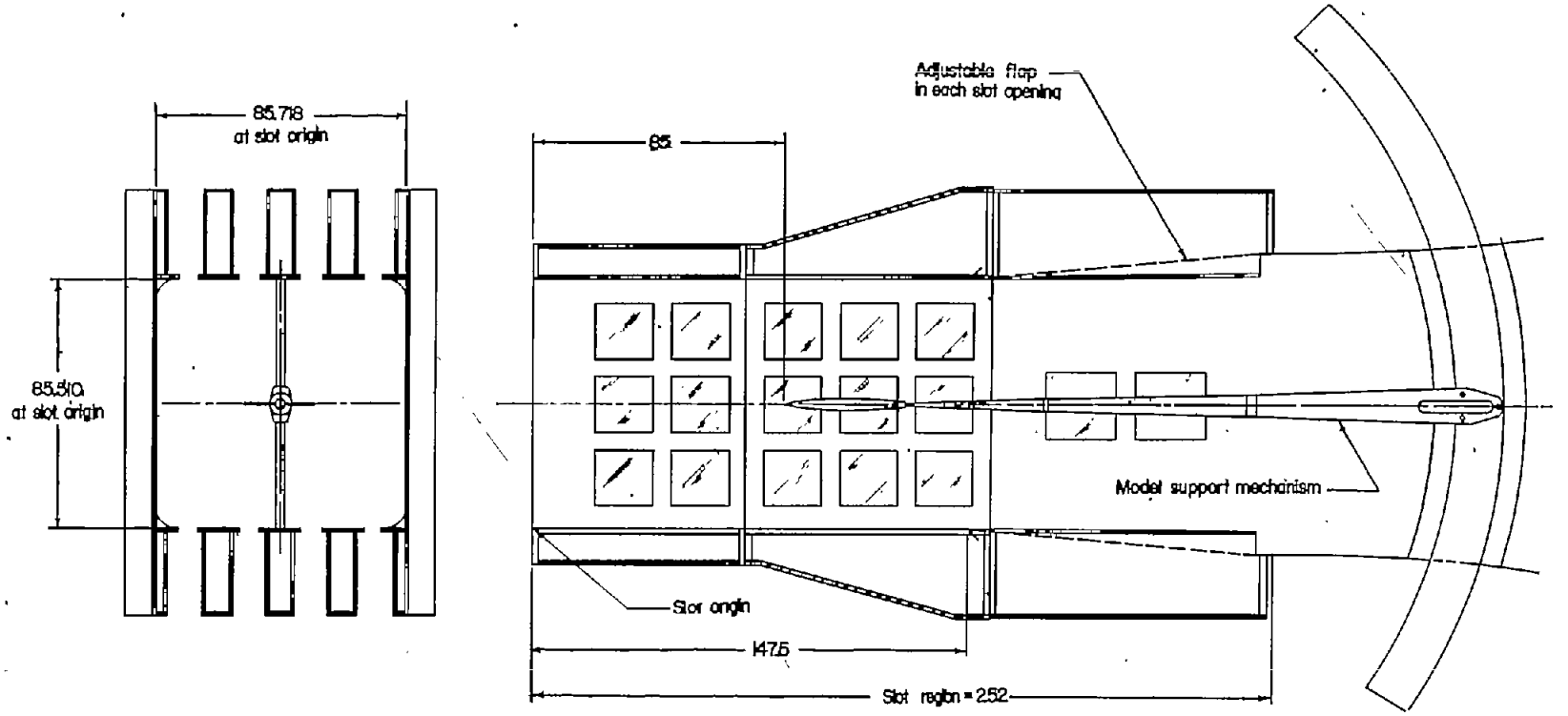

Figure 1.- Details of test section and location of model in the Langley 8-foot transonic pressure tunnel. All dimensions are in inches.

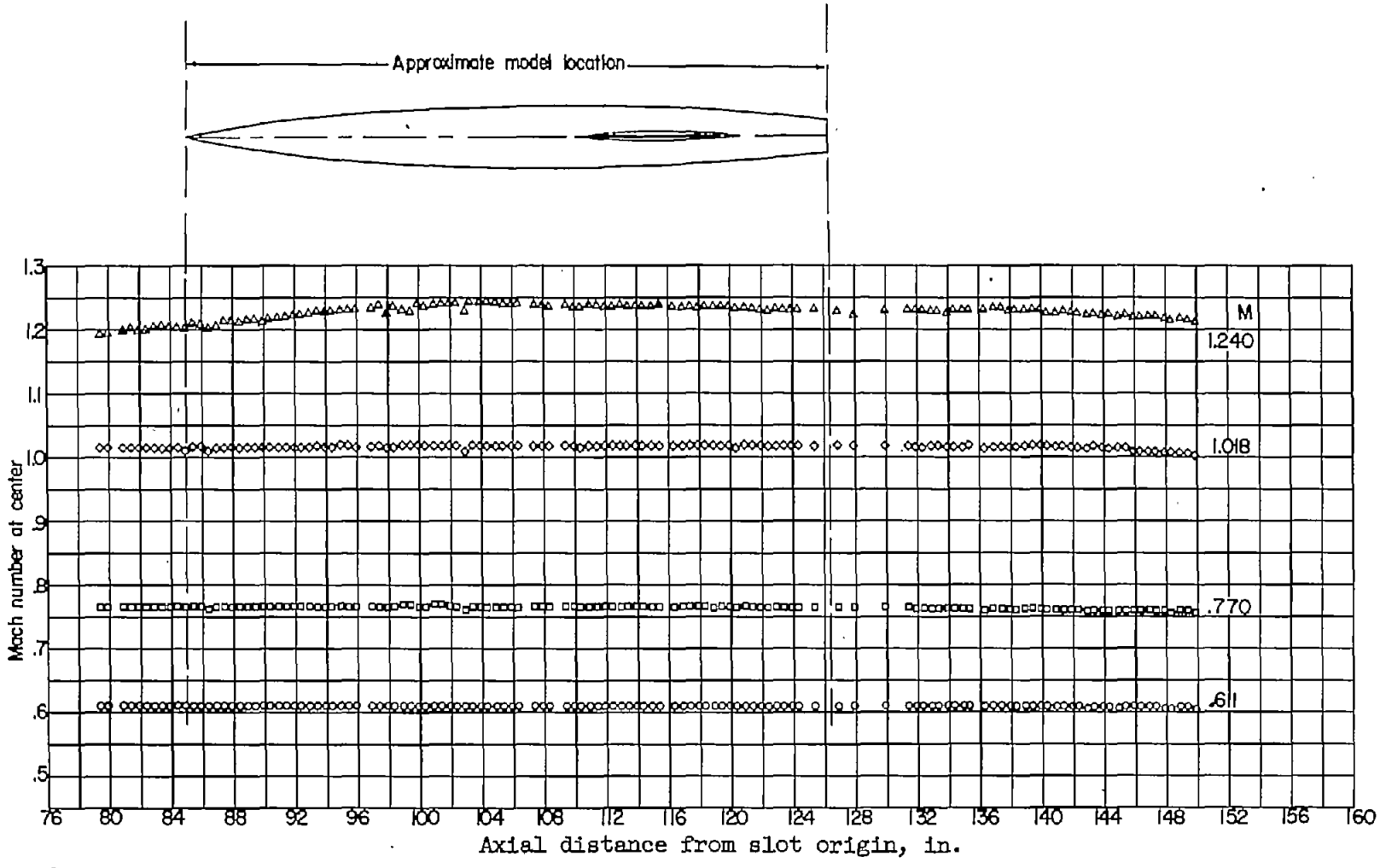

Figure 2.- Typical Mach number distributions in the test section of the Langley 8-foot transonic pressure tunnel.

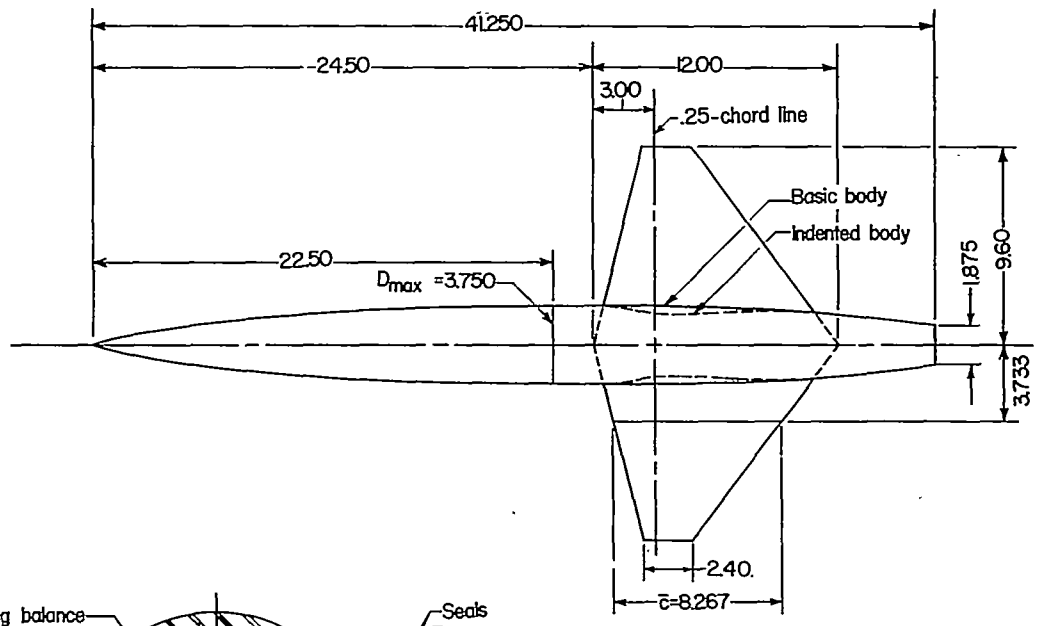

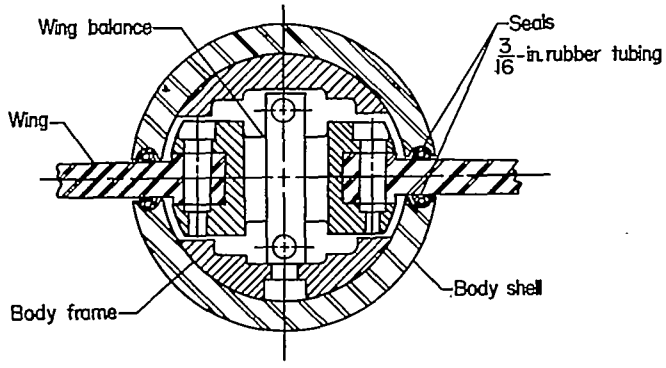

Section showing details of wing balance and seals

Wing

Airfoil section parallel to plane of symmetry: 4-percent-thick symmetrical circular arc, $(t/c)_{max}$ at 0.4c

Aspect ratio	2.67
Taper ratio	.20
Area, sq ft	.96
Dihedral, deg	0
Geometric twist, deg	0
Sweepback of leading edge, deg	14.04

Position of wing on fuselage

Incidence, deg	0
Location of chord plane from fuselage axis, in.	0

Figure 3.- Wing-body configurations tested. All dimensions are in inches except as noted.

[redacted]

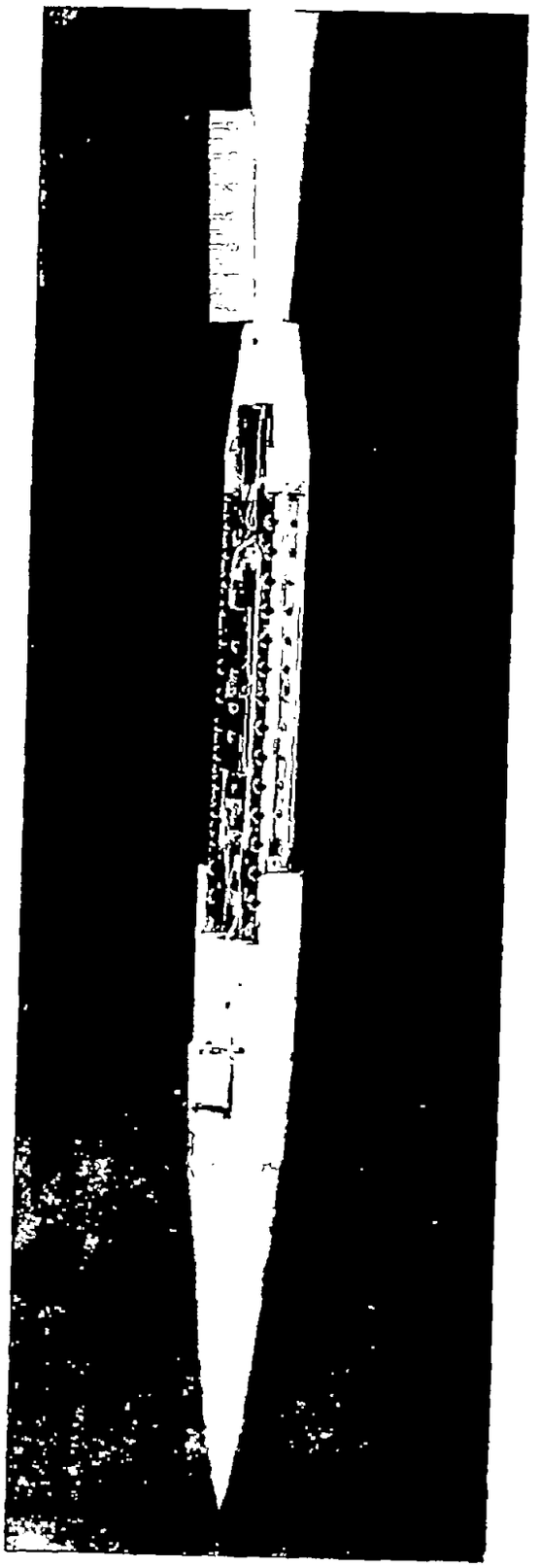

L-84806

Figure 4.- Body frame showing strain-gage balance.

[redacted]

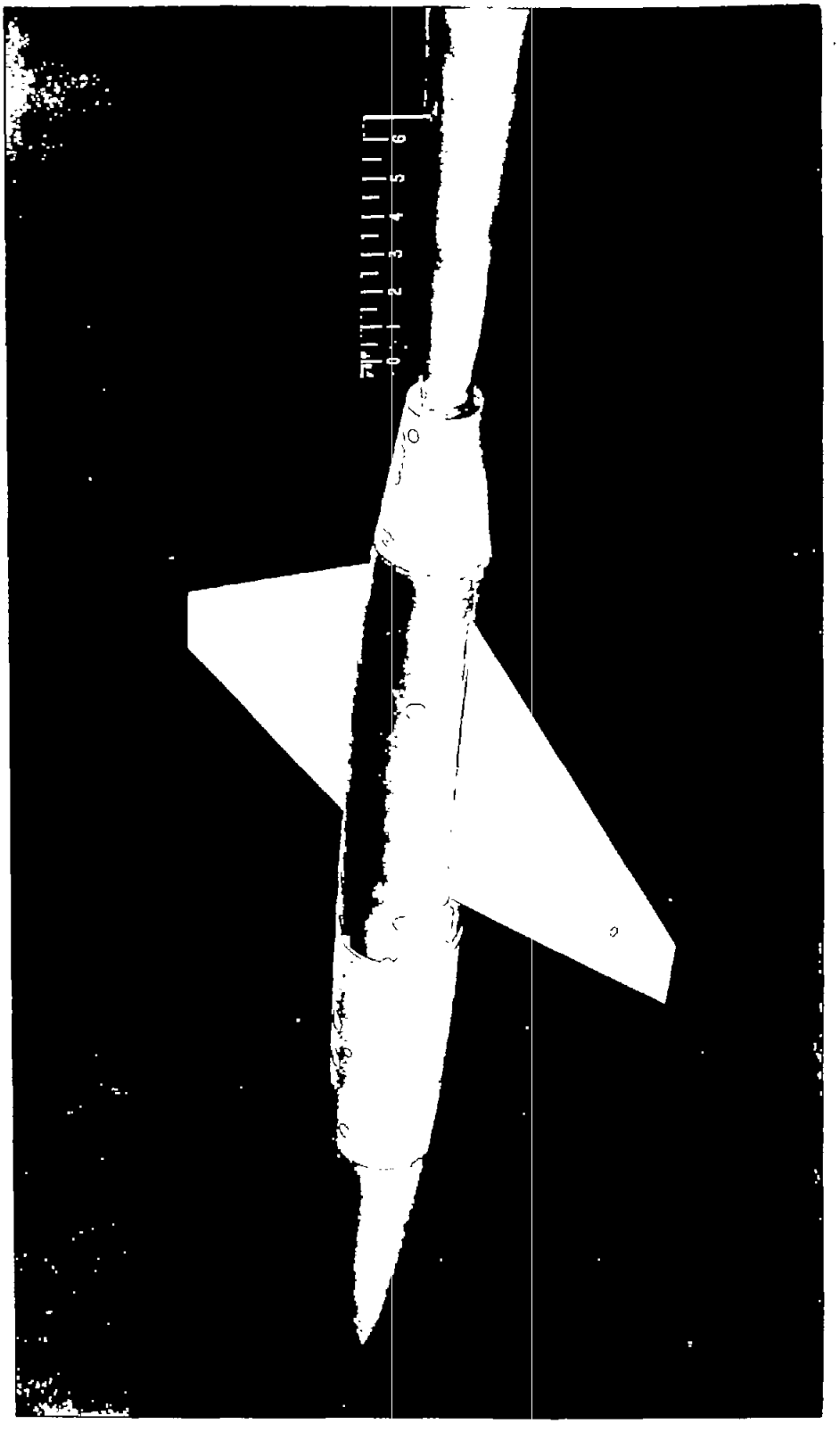

L-84825

Figure 5.- Complete model with basic body.

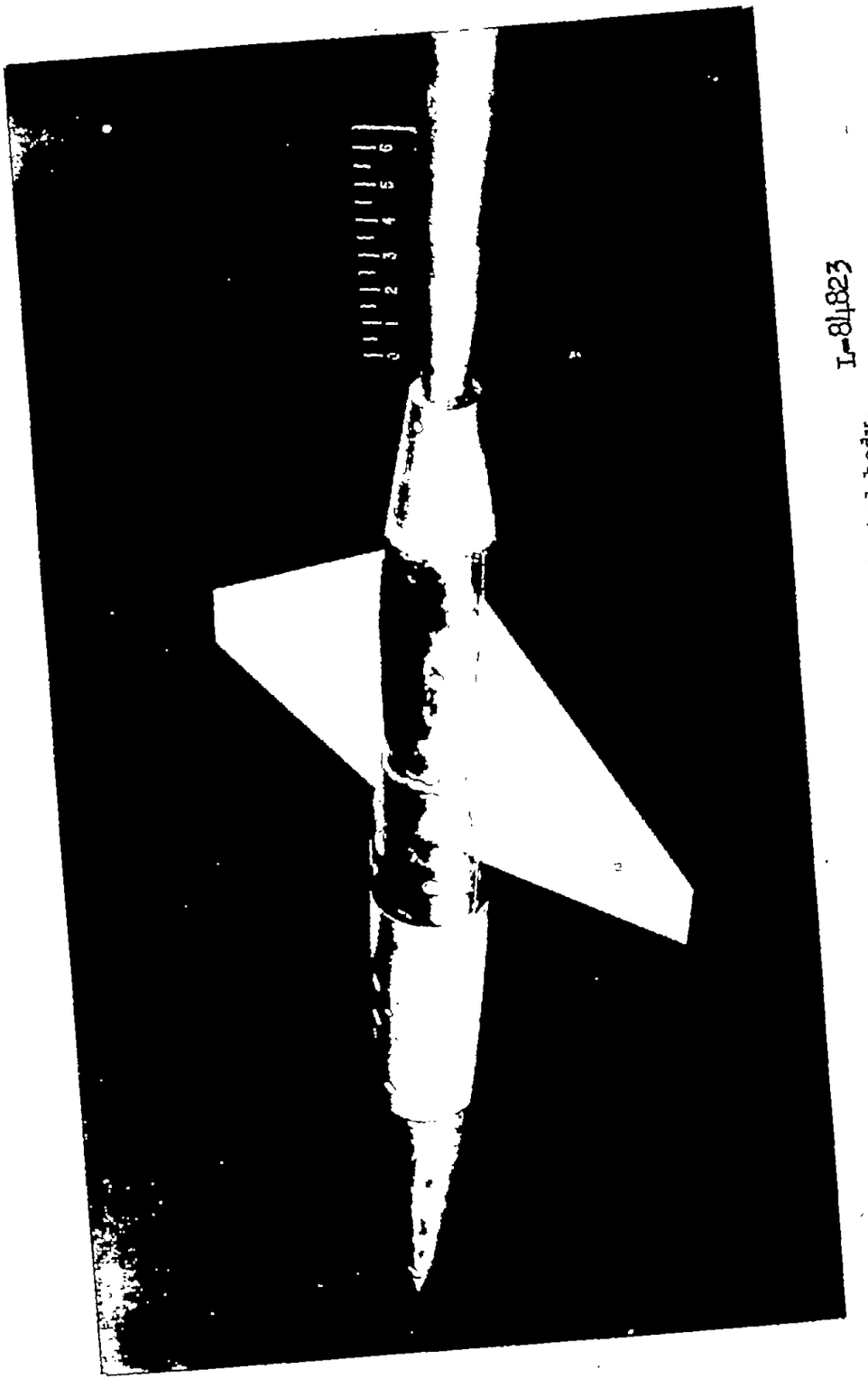

L-84823

Figure 6.- Complete model with indented body.

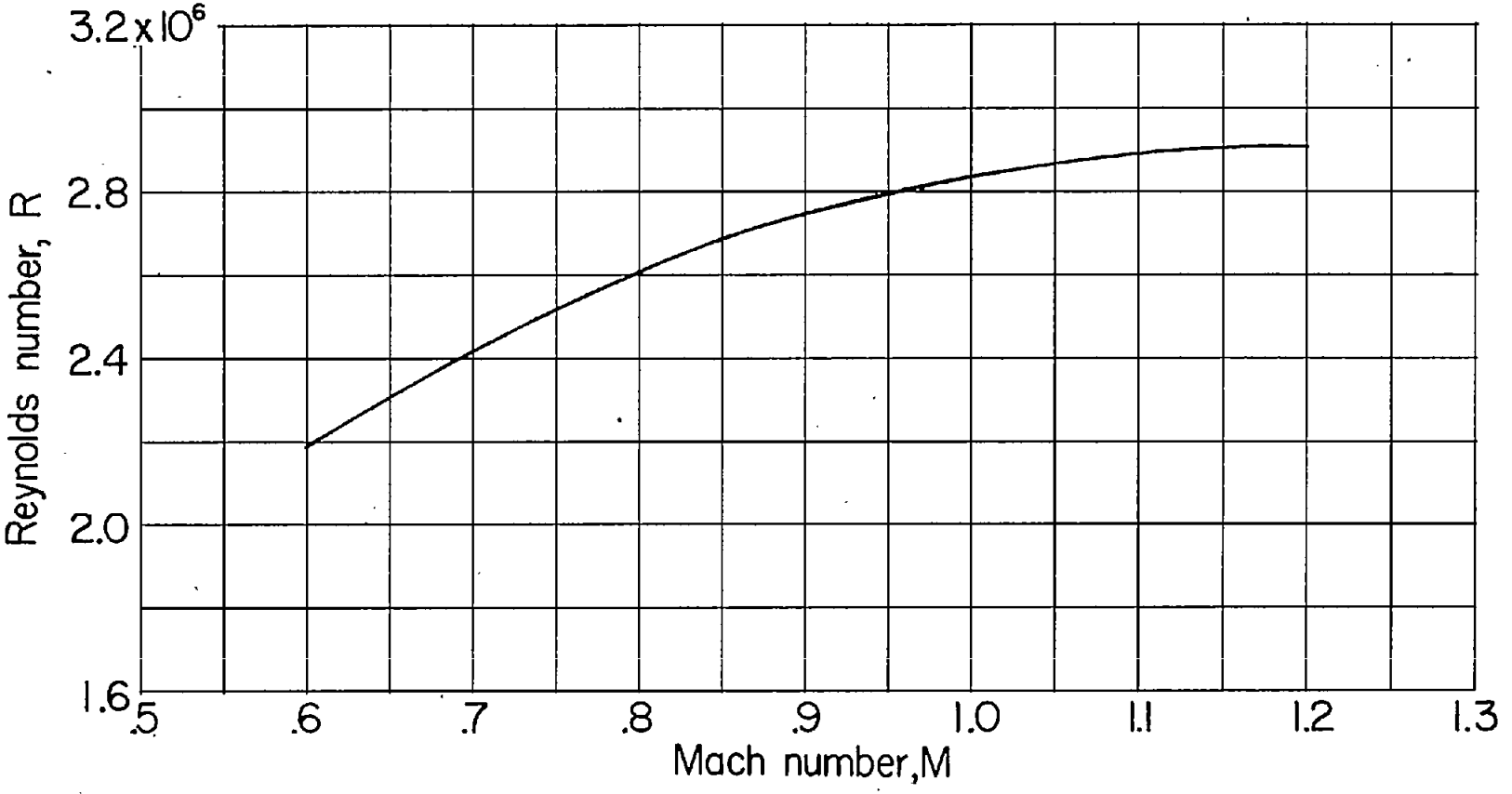

Figure 7.- Variation of Reynolds number with Mach number.

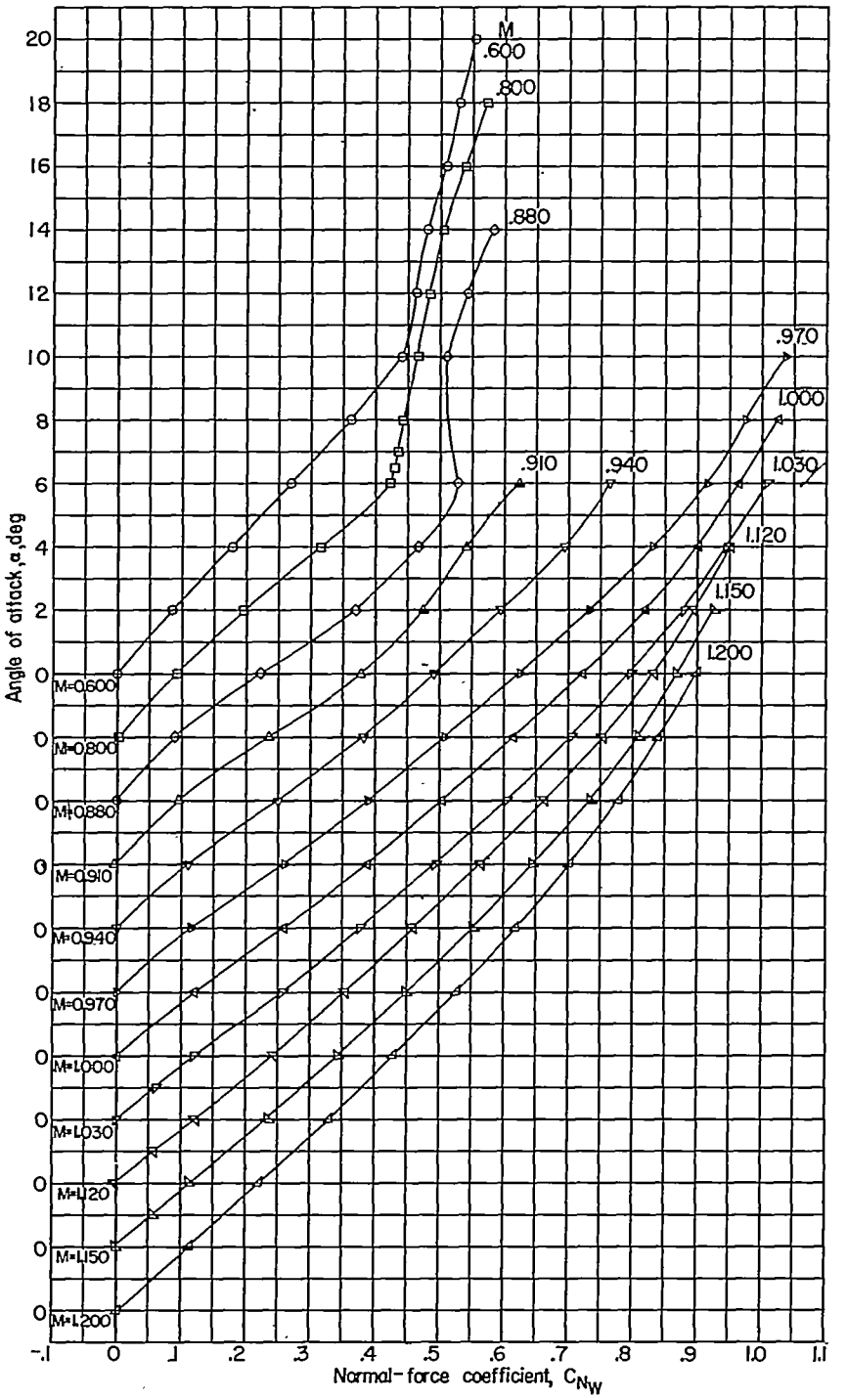

(a) Variation of α with C_{N_W}.

Figure 8.- Aerodynamic characteristics of the wing in the presence of a basic body.

[redacted]

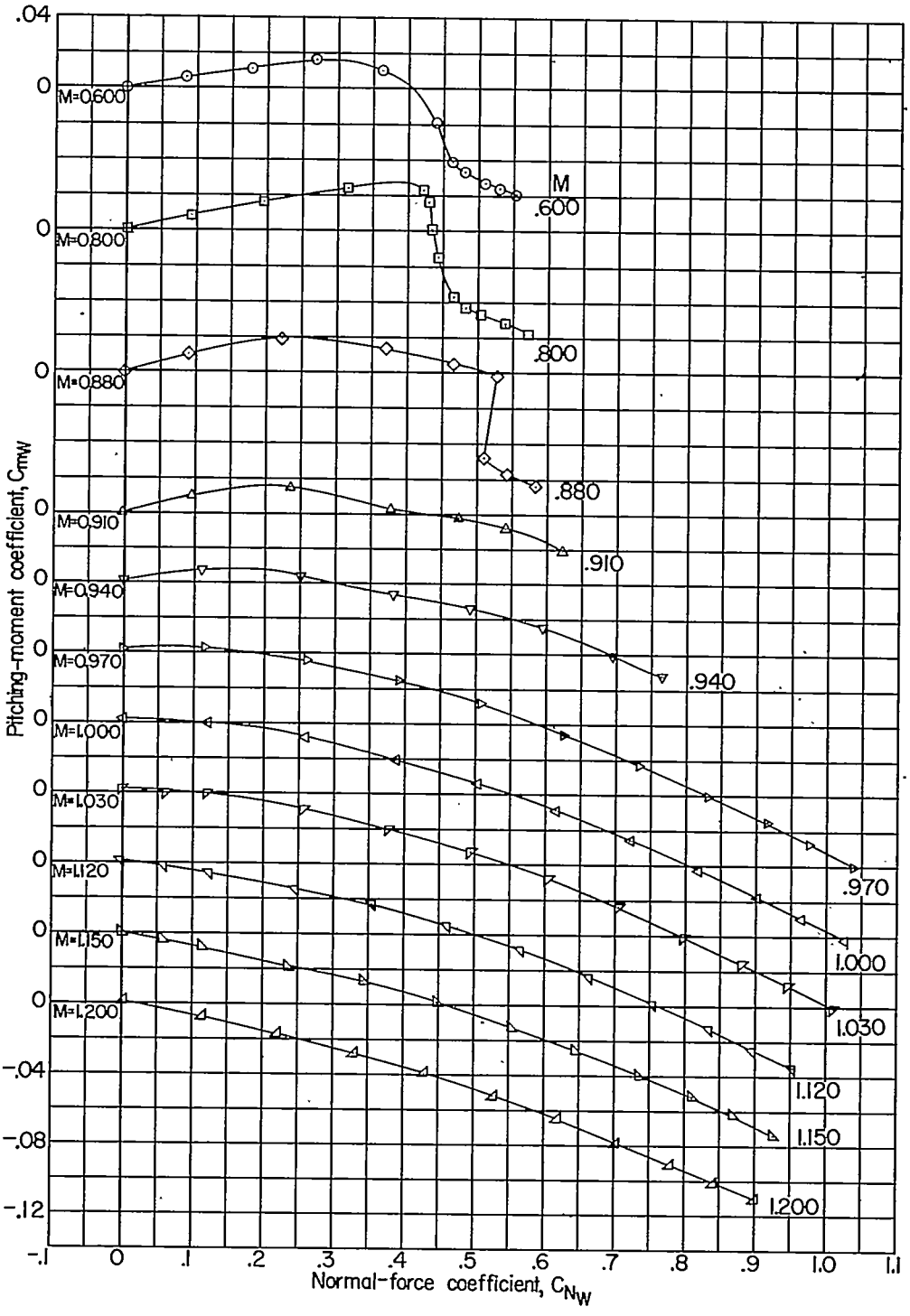

(b) Variation of C_{m_W} with C_{N_W}.

Figure 8.- Continued.

[redacted]

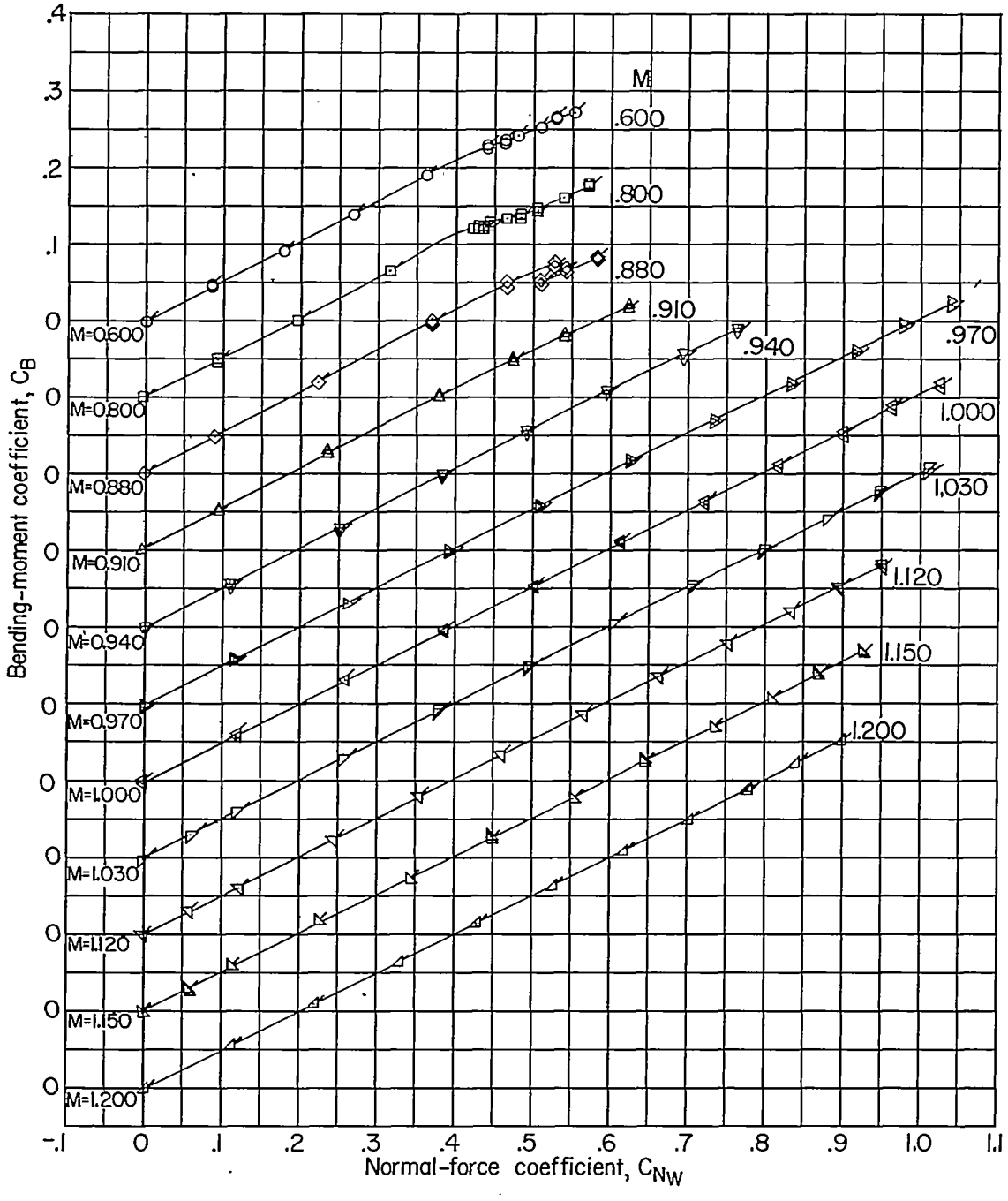

(c) Variation of C_B with C_{N_W} for left and right wing panels. Flagged symbols indicate left wing panel.

Figure 8.- Concluded.

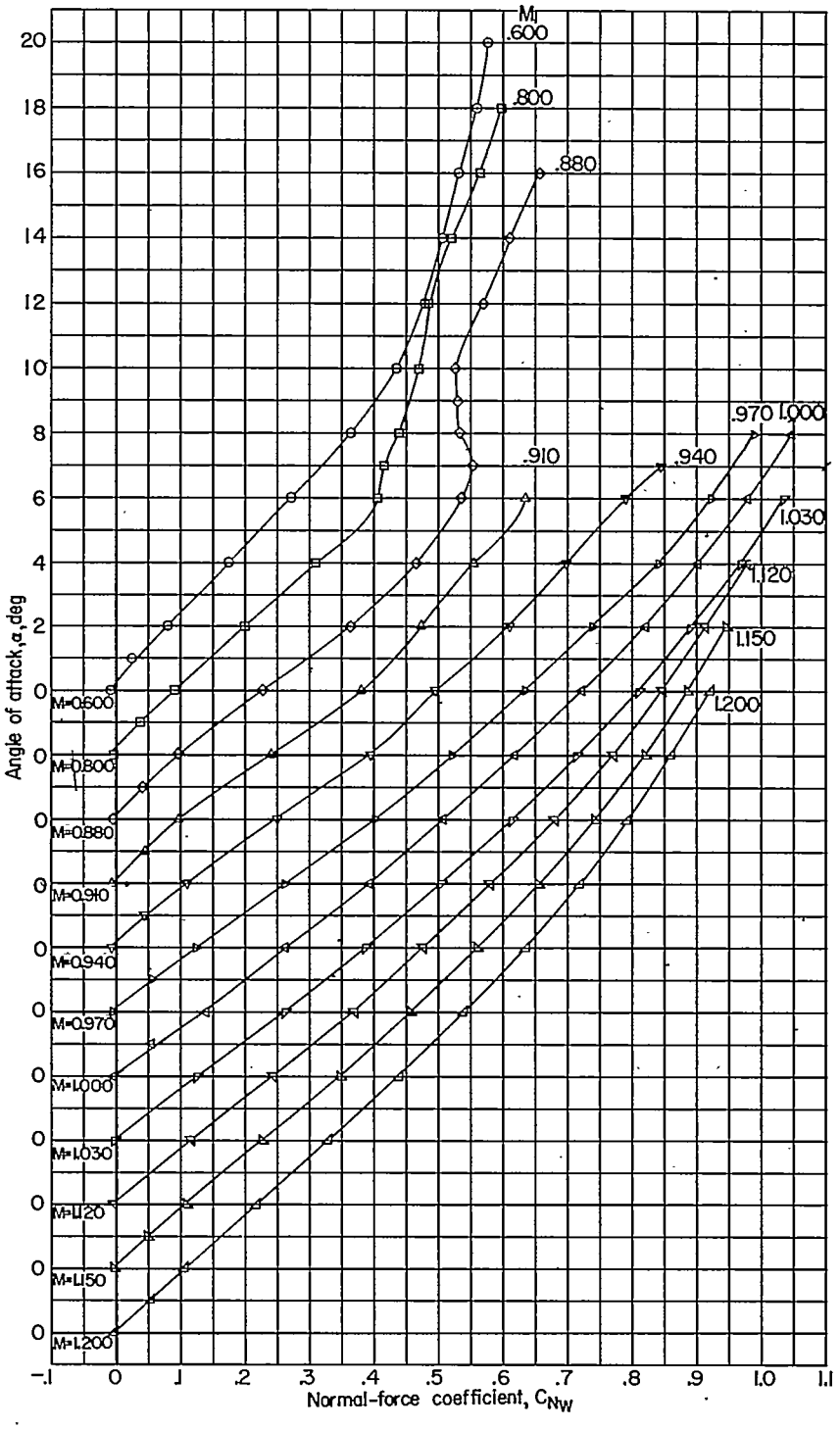

(a) Variation of α with C_{N_W}.

Figure 9.- Aerodynamic characteristics of the wing in the presence of an indented body.

[redacted]

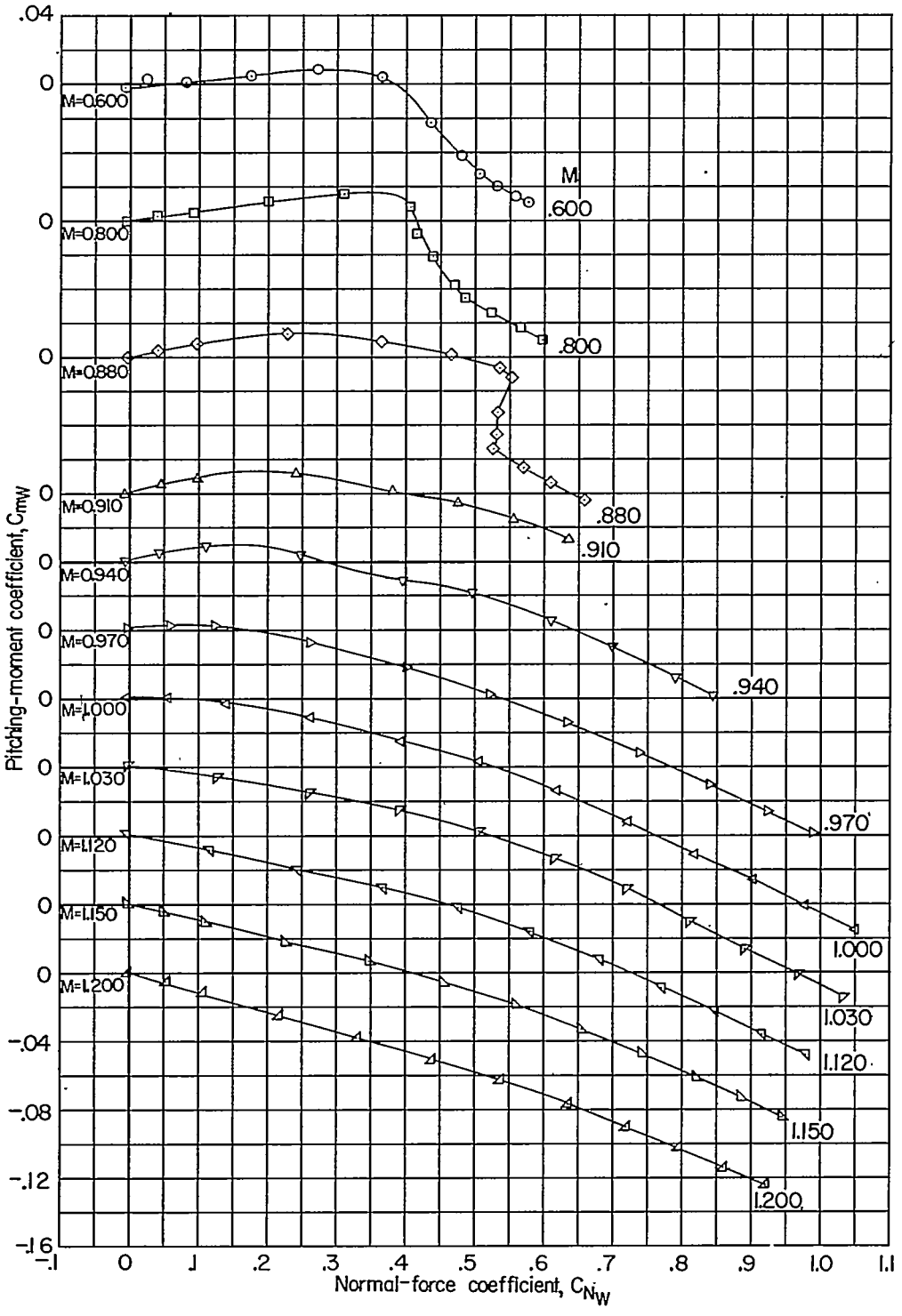

(b) Variation of C_{m_W} with C_{N_W}.

Figure 9.- Continued.

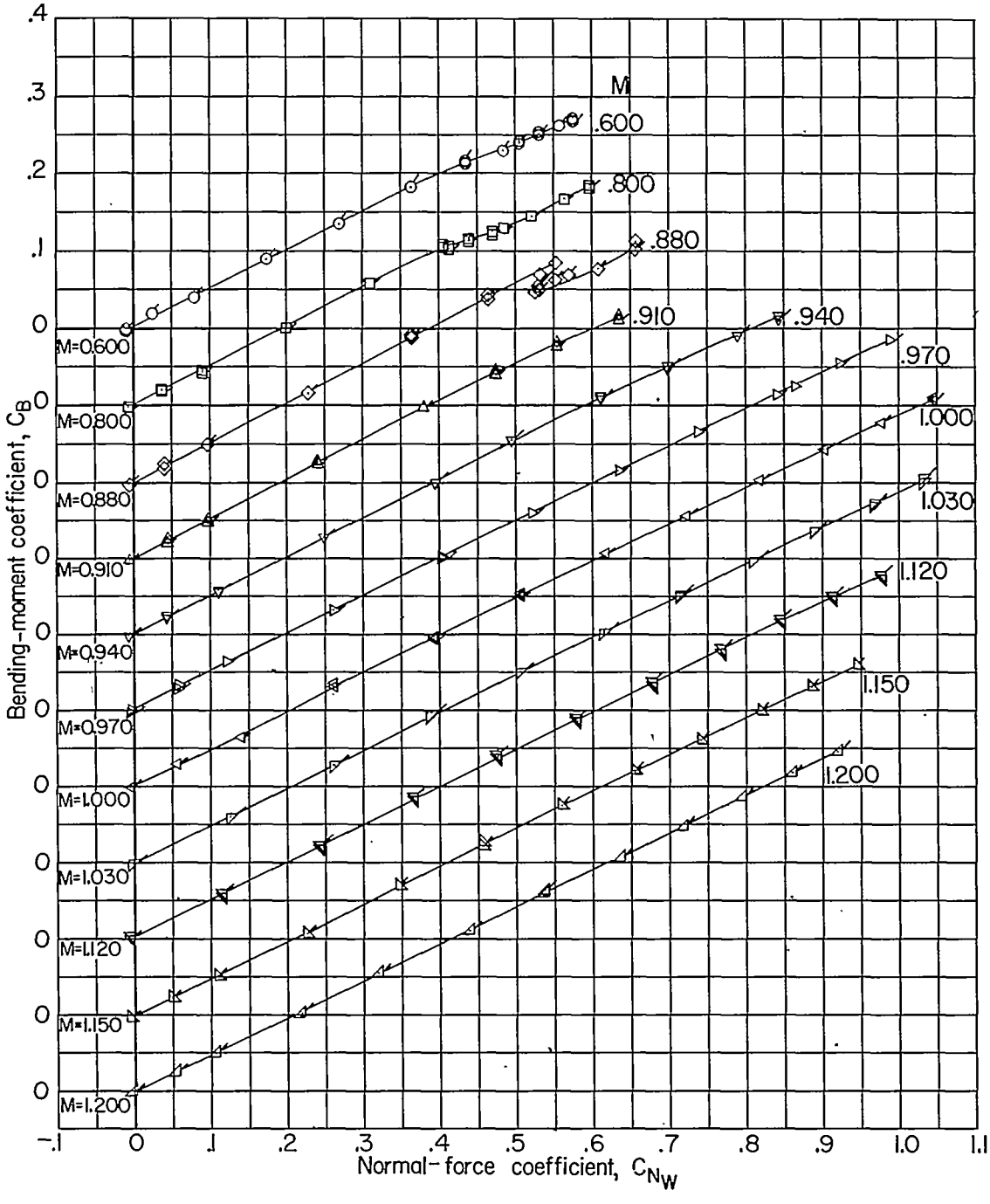

(c) Variation of C_B with C_{N_W} for left and right wing panels. Flagged symbols indicate left wing panel.

Figure 9.- Concluded.

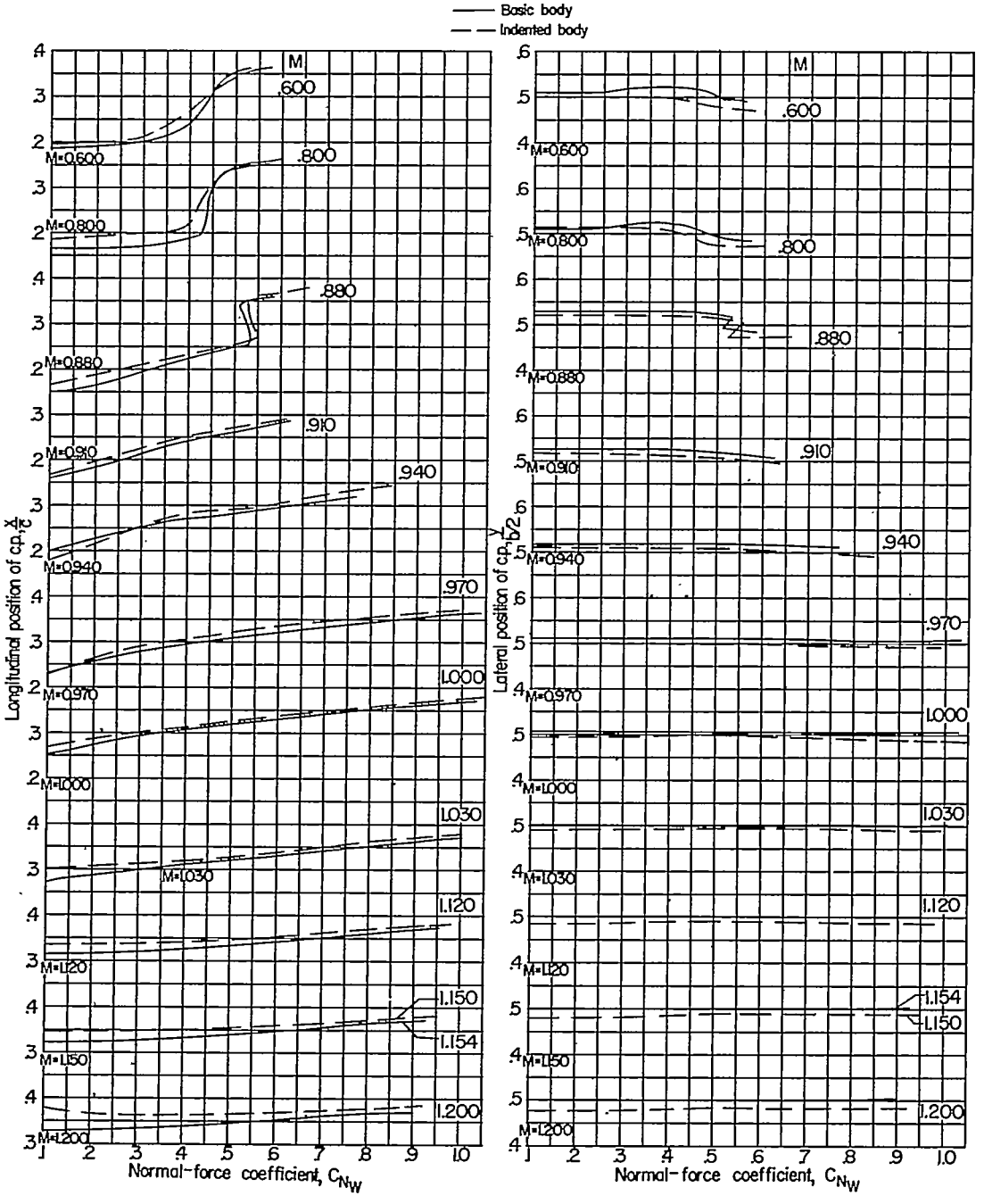

Figure 10.- Effect of body indentation on the variation of the longitudinal and lateral location of the center of pressure with wing normal-force coefficient.

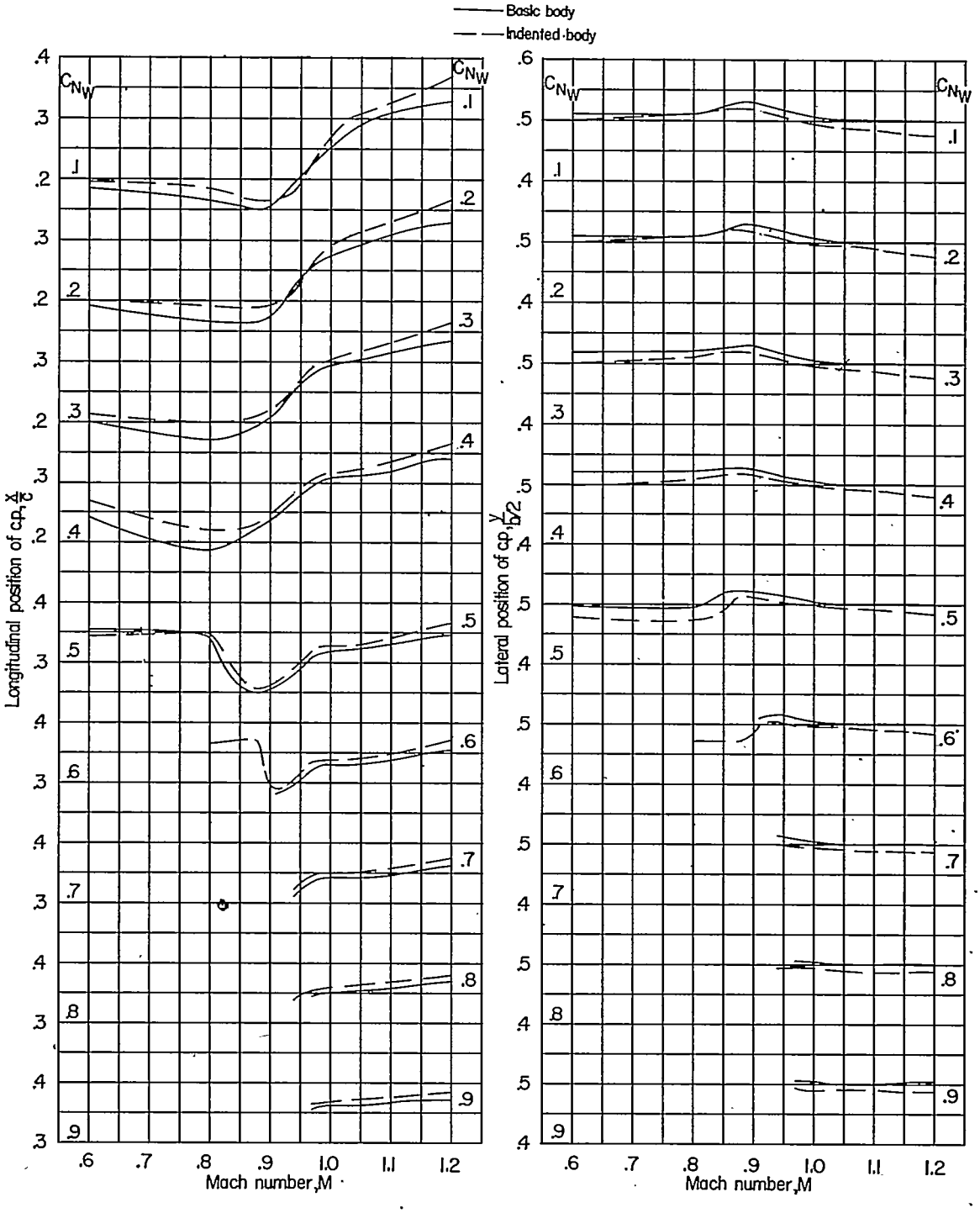

Figure 11.- Effect of body indentation on the variation of the longitudinal and lateral location of the center of pressure with Mach number.

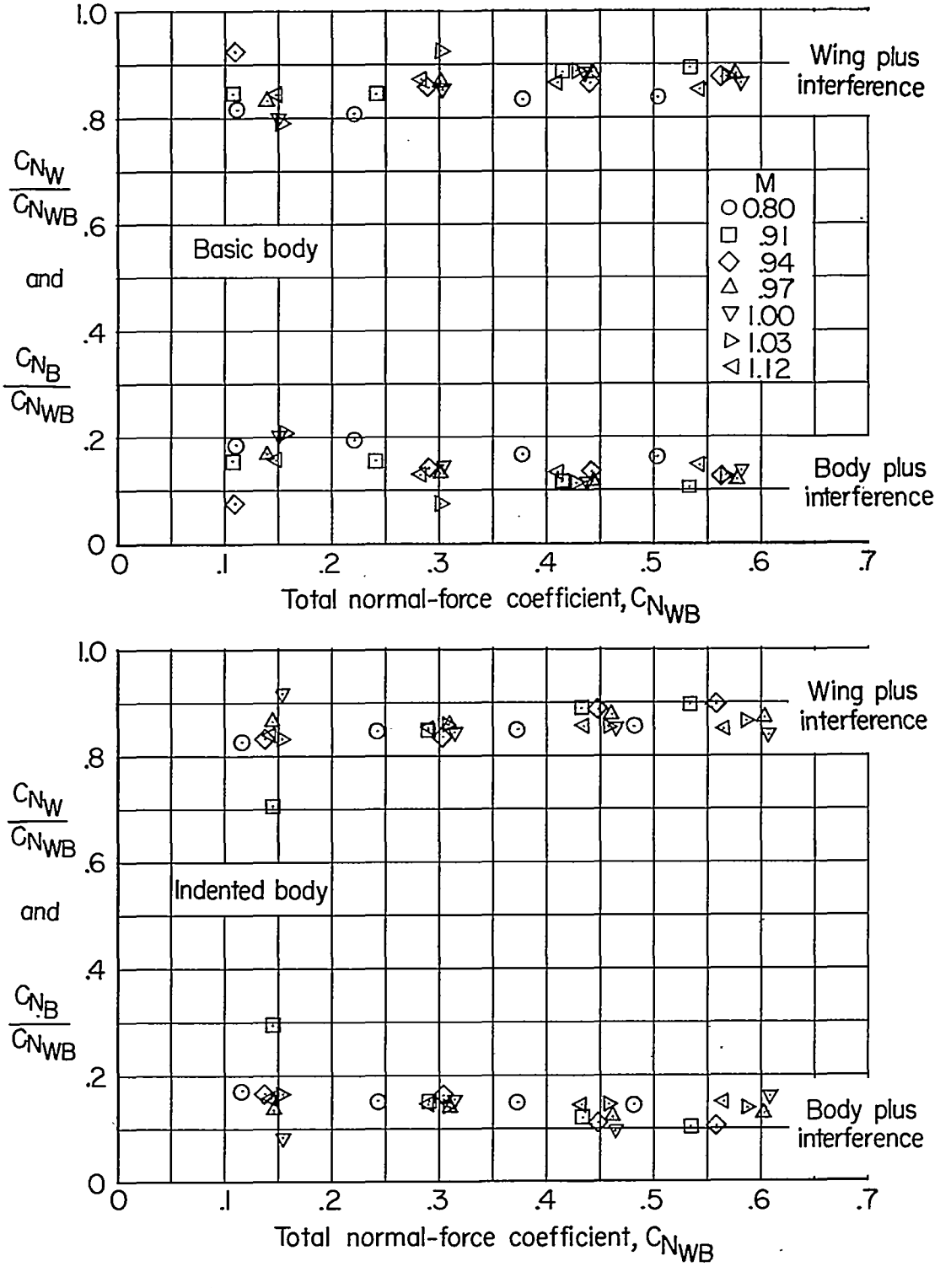

Figure 12.- Division of load between the wing and body.

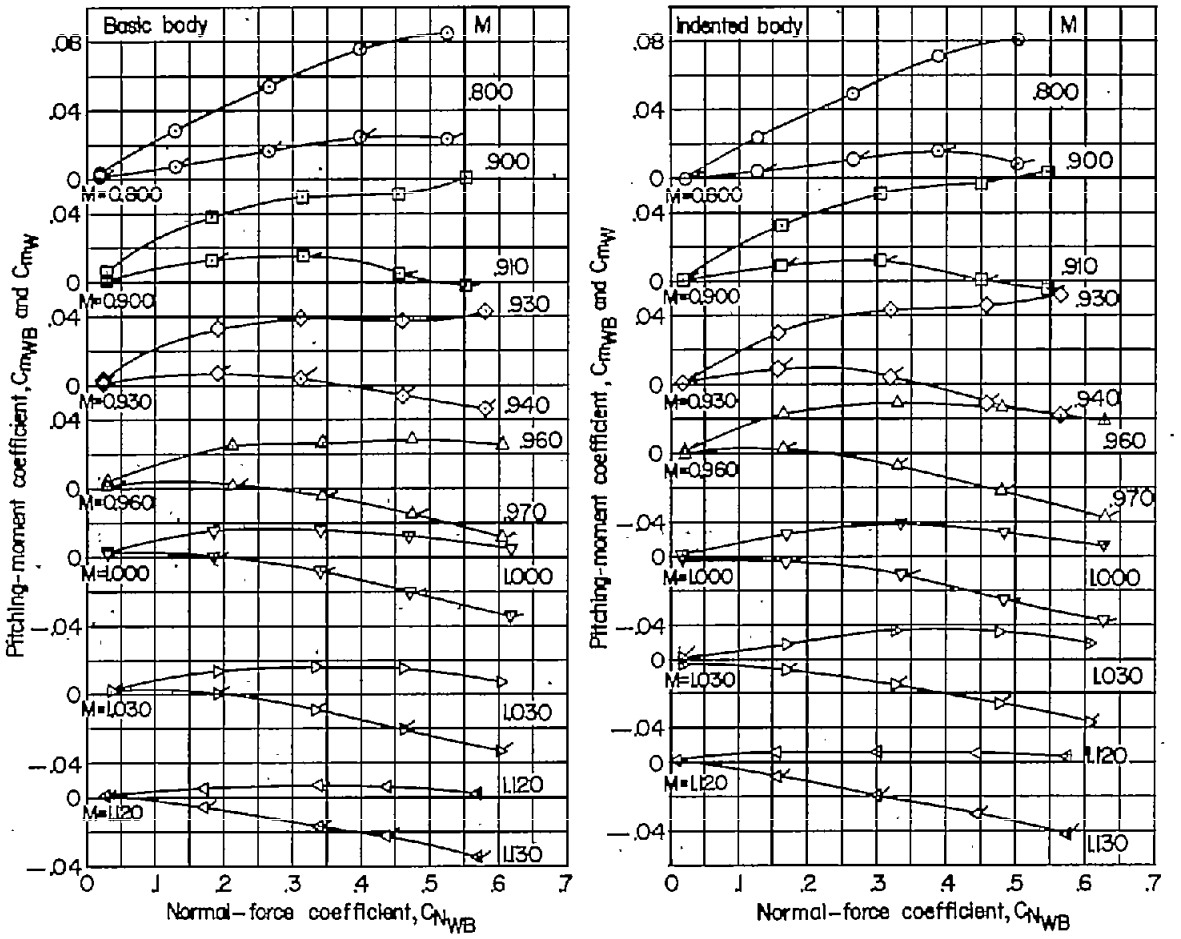

(a) Basic body.

(b) Indented body.

Figure 13.- Variation of pitching-moment coefficient with wing-body normal-force coefficient for the wing-body combination and for the wing in the presence of body. Flags indicate the wing in the presence of the body.

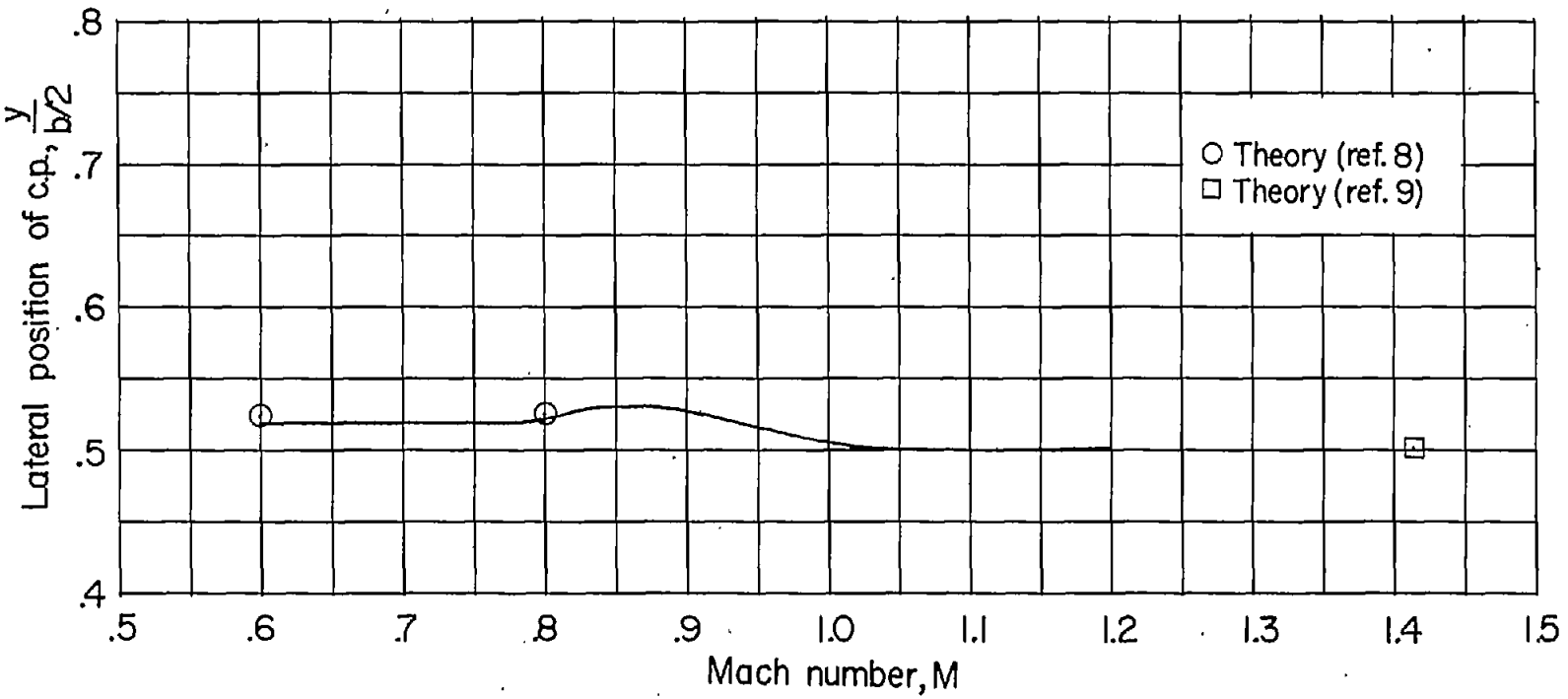

Figure 14.- Comparison of experimental lateral center-of-pressure location with theory. Basic body. $C_{N_W} = 0.3$.